Title
Activation pH and Gating Dynamics of Influenza A M2 Proton Channel Revealed by Single-Molecule Spectroscopy

Permalink
https://escholarship.org/uc/item/7718s39g

Journal
Angewandte Chemie International Edition, 56(19)

ISSN
1433-7851

Authors
Lin, Chun-Wei
Mensa, Bruk
Barniol-Xicota, Marta
et al.

Publication Date
2017-05-02

DOI
10.1002/anie.201701874

Peer reviewed

Activation pH and Gating Dynamics of Influenza A M2 Proton Channel Revealed by Single-Molecule Spectroscopy

Chun-Wei Lin,

Ultrafast Optical Processes Laboratory, Department of Chemistry University of Pennsylvania, Philadelphia, 231 S. 34th Street, Philadelphia, PA 19104 (USA)

Bruk Mensa,

Department of Pharmaceutical Chemistry, University of California San Francisco, 600 16th Street, San Francisco CA 94158-2517 (USA)

Marta Barniol-Xicota,

Department of Pharmaceutical Chemistry, University of California San Francisco, 600 16th Street, San Francisco CA 94158-2517 (USA)

William F. DeGrado, and

Department of Pharmaceutical Chemistry, University of California San Francisco, 600 16th Street, San Francisco CA 94158-2517 (USA)

Prof. Dr. Feng Gai

Ultrafast Optical Processes Laboratory, Department of Chemistry, University of Pennsylvania, Philadelphia, 231 S. 34th Street, Philadelphia, PA 19104 (USA)

Department of Chemistry, University of Pennsylvania, Philadelphia, 231 S. 34th Street, Philadelphia, PA 19104 (USA)

Abstract

Because of its importance in viral replication, the M2 proton channel of the Influenza A virus has been the focus of many studies. While we now know a great deal about the structural architecture underlying its proton conduction function, we know little about its conformational dynamics, especially those controlling the rate of this action. Herein, we employ a single-molecule fluorescence method to assess the dynamics of the inter-helical channel motion of both full-length M2 and the transmembrane domain of M2. We find that the rate of this motion depends not only on the identity of the channel and membrane composition, but also on pH in a sigmoidal manner. For the full-length M2 channel, the rate is increased from $(\sim190\ \mu s)^{-1}$ at high pH to $(\sim80\ \mu s)^{-1}$ at low pH, with a transition midpoint at pH 6.1. Because the latter is within the range reported for the conducting pK_a value of the His37 tetrad, we believe that this inter-helical motion accompanies proton conduction.

Entry for the Table of Contents

Correspondence to: Feng Gai.
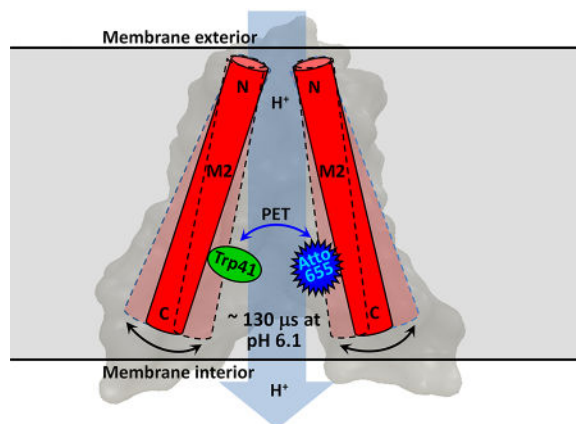
Motion of the gate: The Trp41 gate of the M2 proton channel is shown to undergo a spontaneous conformational motion on a timescale of tens to hundreds of microseconds. The time constant of this motion exhibits a sigmoidal dependence on pH with a midpoint that closely matches the electrophysiologically determined conducting pK_a value of the His37 tetrad, suggesting that this motion accompanies proton conduction.

Keywords

M2 proton channel; Fluorescence correlation spectroscopy; Photoinduced electron transfer; Conformational dynamics; pH titration

The M2 protein of the Influenza A virus consists of 97 residues and exists in the envelope of the virus as a homotetramer.[1] One important function of this M2 tetramer, which forms a pH-responsive channel, is to shuttle protons unidirectionally across the viral membrane, allowing acidification of the viral interior in the endosome lumen.[1,2] Because this acidification event plays a key role in viral replication, the M2 proton channel has become a popular anti-viral drug target.[3] As such, many studies have been devoted to elucidating its proton conduction and inhibition mechanisms.[4–8] In particular, significant progress has been made in recent years in structure-based studies,[9] providing much needed molecular insight into the understanding of the pH-activated, asymmetric proton conducting action of the M2 proton channel. While the details of existing models[10–19] differ with regard to the mechanism of proton conduction, they share several common features: (1) proton selection and channel activation are primarily controlled by the His37 tetrad (Supporting Information, Figure S1); (2) the channel is activated or transitioned from a closed to an open state when three His37 residues are protonated at an acidic pH, (3) the role of the Trp41 tetrad (Supporting Information, Figure S1) is to allow unidirectional proton conduction only when the pH is low on the outside of the virus, and (4) channel waters are actively involved in proton conduction. Although we now know a great deal about the structure of this membrane-spanning channel and many thermodynamic aspects of its mechanism of action, we know relatively little about the underlying dynamics that control the rate of proton conduction. Herein, we aim to address this question by using a single-molecule fluorescence technique to assess the inter-helical conformational dynamics of the M2 channel in model membranes.

As a necessary process for proton conduction, the protonation-deprotonation event of His37 could be the rate-limiting step.[13,17] However, the study of Hong and coworkers[20] found that the His37-water proton exchange rate (~10^5 s^{-1}) is significantly higher than the time-averaged unitary proton flux of M2, suggesting that in addition to the essential and rapid protonation-deprotonation step allowing the passage of a proton through the His37 gate,[21,22] additional steps need to be included in the kinetic mechanism in order to explain the observed rate of proton conduction. In fact, several scenarios have been proposed, including (1) the His37-Trp41 cation-π interaction can periodically form and break at low pH,[23] thus modulating the rate of proton conduction, (2) a recycling step is required after each proton release,[24] which involves closing the Trp41 gate and opening the Val27 gate and hence decreases the rate of proton conduction, (3) even at low pH the C-terminal open conformation (i.e., the conformation that allows transfer of protons from His37 to the interior of the virus) is only transiently populated,[25] leading to a slower apparent rate, and (4) proton migration from water cluster B to C (Supporting Information, Figure S1) requires an additional conformational transition that involves Trp41 via either sidechain or backbone motions.[26] Given that Trp41 is involved in all these scenarios, we carried out a single-molecule fluorescence experiment to directly assess its conformational dynamics under equilibrium but different pH conditions using both the full-length M2 protein and a truncated variant corresponding to the transmembrane domain of M2 (referred to as M2TM).

Our experimental design is based on the notion that Trp can effectively quench the fluorescence of oxazine dyes, such as Atto 655.[27,28] Because this quenching effect arises from a photoinduced electron transfer (PET) process, it requires the quencher (Trp) to be sufficiently close to the fluorophore (dye). In addition, as the rate of PET is sensitively dependent on the quencher-fluorophore separation distance (R_{QF}), it is possible to utilize a Trp-dye pair and fluorescence correlation spectroscopy (FCS) to characterize the rate of a specific protein conformational motion; as long as this motion modulates R_{QF} and hence induces fluctuations in the fluorescence intensity.[29,30] To employ this PET-FCS strategy to assess the conformational dynamics of Trp41 in the full-length M2 and M2TM proton channels, we introduced an Atto 655 dye at position 40 via a Cys residue using a double mutant of the respective native sequence, Leu40/Cys-Trp41/Phe (the labeled peptide and protein are hereafter referred to as M2TM* and M2*, respectively). The reason that we use a Trp41/Phe M2 (M2TM) mutant to carry the Atto 655 fluorescence reporter is to eliminate the intra-molecular quenching effect arising from the Trp residue on the same helix in the tetramer, which, when present, would dominate the observed PET-FCS signal.[31] To use M2* (M2TM*) to report the motion of Trp41, we use a mixture of wild-type M2 (M2TM) and M2* (M2TM*) to prepare the corresponding membrane-bound tetramers. By specifically controlling the ratio between the labeled and non-labeled proteins (peptides), we ensure that the large majority of tetramers prepared contain either no or only one M2* or M2TM*. Because in a M2* (M2TM*) containing tetramer only an inter-molecular quenching effect can occur, the PET-FCS signal thus provides a direct measurement of the underlying Trp41 dynamics. Our results show that Trp41 is subject to a conformational motion that occurs on a timescale of tens to hundreds of microseconds, depending on pH, membrane composition, and the identity of the proton channel (i.e., full-length M2 or M2TM). To the best of our knowledge, this is the first study revealing that the M2 proton

channel undergoes a spontaneous conformational fluctuation on the long microsecond timescale in bilayers.

As described in the experimental section, a M2*/M2 (M2TM*/M2TM) ratio of 1/50 was used to prepare the membrane-bound tetrameric protein (peptide) samples. Therefore, most of the tetramers would not contain any M2* (M2TM*) and hence will not contribute to the FCS signal. Furthermore, this low molar ratio makes the percentage of the tetramers that contain more than one M2* (M2TM*) molecule significantly smaller than that containing only one M2* (M2TM*) (i.e., 0.04% versus 2%). For ease of discussion, below we refer to these fluorescent tetramers as M2*-M2 (M2TM*-M2TM) channels. In addition, we used two model membranes, in the form of large unilamellar vesicles (LUVs), composed of POPC/POPG (4/1) and POPC/POPG/Cholesterol (4/1/2), respectively.

First, we examined the Trp41 conformational dynamics in a truncated version of the M2 proton channel, the M2TM channel. Previous studies[6,17,20,26,31–37] have shown that the tetrameric assembly, proton conduction ability and drug binding property of the M2 channel are maintained in the M2TM channel. Thus, this model M2 channel has become a popular system for interrogating the structural and dynamic determinants of M2 function. As shown (Supporting Information, Figure S2), the FCS curve obtained with M2TM*-bound POPC/POPG LUVs can be well fit by Eq. (1) with a τ_D of 4.1 ms and a single dynamic component of 5.1 μs (amplitude = 0.15).

$$G(\tau) = \frac{1}{N} \cdot \left(\left(\frac{1}{1 + \frac{\tau}{\tau_D}} \right) \cdot \left(\frac{1}{1 + \frac{\tau}{\omega^2 \tau_D}} \right)^{1/2} \right) \times \left(\frac{1 - \sum\limits_{i=1}^{m} \left(T_i - T_i \cdot \exp\left(-\frac{\tau}{\tau_i} \right) \right)}{1 - \sum\limits_{i=1}^{m} T_i} \right) \quad (1)$$

The τ_D value is consistent with the diffusion correlation time of 100-nm-sized LUVs under our experimental conditions, whereas the 5.1 μs dynamic component can be assigned to triplet state formation of the fluorescence reporter based on previous FCS measurement on the Atto 655 dye.[31,38] In comparison (Supporting Information, Figures S3 and S4), besides these two components, the FCS curve obtained with M2TM*-M2TM channels at pH 5.0 contains an additional dynamic component with a time constant of 121 μs. Therefore, this FCS component must originate from PET and, because only inter-molecular PET can occur, its time constant (hereafter referred to as τ_{PET}) manifests the conformational changes of the channel that influence the separation distance between the Atto 655 reporter on one helix and Trp41 residues on the other three.

As shown (Figure 1 and Supporting Information, Table S1), the τ_{PET} of M2TM*-M2TM in POPC/POPG membranes exhibits a sigmoidal dependence on pH with a midpoint of 6.8 ± 0.1. Because the fluorescence spectra of the M2TM* peptide measured at pH 5.0 and 7.0 are practically identical (Supporting Information, Figure S5), this pH dependence is unlikely due to the Atto 665 dye, but instead arises from the conformational motions of the channel. Interestingly, adding cholesterol to the model membranes has a notable effect on τ_{PET} as well as its pH dependence (Figure 1; Supporting Information, Figures S6 and S7 and Table

S1). It is clear that in the presence of cholesterol the value of τ_{PET} becomes longer and the midpoint of the corresponding pH titration curve is decreased to 6.3 ± 0.2.

The observed PET signal could arise from either the Trp41 sidechain (local) motion or an inter-helical (global) motion. To distinguish between these two possibilities, we carried out a control experiment using a dye-labeled channel wherein only intramolecular PET can occur. Specifically, we introduced the Atto 655 dye through a Leu40/Cys mutant of M2TM (the labeled peptide is hereafter referred to as M2TM**) and then mixed M2TM** with a Trp-less mutant of M2TM, i.e., Trp41/Phe, at a 1/50 ratio in LUV membranes composed of POPC/POPG/Cholesterol (4/1/2). As shown (Supporting Information, Figures S8 and S9), the FCS curves obtained with M2TM**-Trp41/Phe M2TM channels at both pH 5.0 and 7.0 can be well fit by only one kinetic component ($m = 1$) with a time constant of a few μs, which corresponds to the aforementioned triplet state formation. Thus, this result indicates that the Trp41 sidechain motion occurs on a timescale that is outside of our experimental time window (i.e., faster than μs), consistent with previous studies,[39,40] and that the PET component observed in the case of M2TM*-M2TM is a manifestation of its inter-helical motion.

The effect of cholesterol on τ_{PET} and its pH dependence also supports the above assessment. Many studies have shown that cholesterol can affect the rigidity of lipid membrane and help maintain the structural integrity of the cell membrane.[41–45] Moreover, Cristian *et al.* have shown that cholesterol is critical to the stability of the tetrameric structure of the M2 proton channel.[46] Therefore, it is expected that cholesterol will affect the inter-helical motion of the M2TM channel, as observed. Furthermore, the finding that τ_{PET} becomes shorter at lower pH is in line with previous studies showing that the M2 channel exhibits higher conformational plasticity at acidic pH.[17,23,47,48]

The His37 tetrad can sample four protonation states (i.e., His^{1+}, His^{2+}, His^{3+}, His^{4+}) depending on pH, and the transition from the His^{2+} to His^{3+} state is believed to dictate the closed-to-open transition of the channel.[37] As such, several studies[20,37,49–51] have attempted to determine the underlying pK_a value of this transition. For example, Okada *et al.* reported a pK_a of 5.9 for a truncated variant of M2 (i.e., from residue 25 to 43) in a POPE/POPS (1/1) membrane,[49] whereas a value of 6.3 was determined by Cross and coworkers for M2TM in a DMPC/DMPG (4/1) membrane.[37] Similarly, Pielak and Chou found a pK_a of ~6.6 for the 18–60 segment of M2 in membranes extracted from *E. coli*.[18] However, Hu *et al.* found that in a virus-mimetic membrane consisting of DPPC/DPPE/Cholesterol/SM (21/21/30/28) the pK_a value of this transition for M2TM is decreased to 4.9.[20] Clearly, these studies indicate that the pK_a value governing the His^{2+} to His^{3+} transition of M2TM depends on membrane composition. Thus, considering the fact that a similar dependence is observed for the pH titration curve of τ_{PET} and that the midpoint of this curve is similar to the pK_a value reported by Cross and coworkers,[37] we believe that τ_{PET} is a judicious reporter of the pH-induced conformational changes underlying the closed-to-open transition of the M2TM proton channel. To further validate this notion, we performed FCS measurements on a M2TM channel that does not have proton selectivity. Specifically, based on the whole-cell patch clamp experiment of Wang *et al.*,[52] which showed that mutation of His37 to Gly eliminates the pH dependence of the proton conduction rate of M2, we

assembled channels using M2TM* and the His37/Gly mutant of M2TM in membranes consisting of POPC/POPG/Cholesterol (4/1/2). As indicated (Figure 1; Supporting Information, Figures S10 and S11), the τ_{PET} of this M2TM mutant channel becomes pH independent within the pH range of the experiment and hence corroborates the conclusion reached above. In addition, this finding provides further supporting evidence that the pH-dependence of the PET time constant observed for M2TM*-M2TM does not arise from the Atto 665 dye. Finally, to verify that the mutations used to construct the M2TM*-M2TM channels do not significantly change the proton conduction functionality of the channel, we also carried out proton flux measurements following a protocol previously published by Ma et al.[32] As shown (Supporting Information, Figure S12), the cumulative proton flux per M2TM*-M2TM tetramer (and the corresponding dye-less tetramer) at pH 5.0 was determined to be 7.9 ± 0.7 H+/s, which is almost identical to that (8.6 ± 0.9 H+/s) reported previously for the wild-type M2TM.[26]

With the experimental approach validated, we use it to further study the conformational dynamics of the full-length M2 proton channel. As shown (Supporting Information, Figures S13 and S14), the FCS curve obtained with M2*-M2 channels embedded in the membrane of LUVs consisting of POPC/POPG/Cholesterol (4/1/2) at pH 5.0 contains the expected PET component with a time constant of 84 μs. Similar to that observed for M2TM*-M2TM, the PET time constant of M2*-M2 shows a sigmoidal dependence on pH (between 5 and 8) with a midpoint value of 6.1 ± 0.2 (Figure 2; Supporting Information Table S1). This pH value is consistent with that obtained from both whole-cell patch clamp and liposome experiments,[52–54] which showed that the effective pK_a for proton conduction is ~6. For M2TM, the pK_a value varies by 0.5 pH unit in the presence versus absence of cholesterol. By contrast, the pK_a values measured for M2TM*-M2TM versus M2*-M2 in the same lipid compositions are nearly identical within the experimental error. Thus, it is likely that the differences in pK_a, which are sometimes attributed to differences in the length of a given protein construct[37] are, instead, at least partially attributable to the differences in lipid compositions used in the different studies. Moreover, when comparing to the PET dynamics of M2TM*-M2TM, those of M2*-M2 is faster at both high and low pH values. These results indicate that the Trp41 tetrad in the full-length proton channel undergoes a faster conformational fluctuation than that of the truncated version. This increase in the rate of the inter-helical conformational dynamics likely results from subtle differences in the packing of the tetrametric structures of the full-length and truncated M2 channels.[4],[9]

The M2 channel has a relatively low proton conductance rate, which is in the range of 10^1–10^4 protons/s.[55–57] This value is one to three orders of magnitude slower than that expected for the transmission of a proton through a water-filled pore of the size of the M2 channel devoid of ionizable groups.[58] While it is well recognized that the His37 tetrad poses a barrier for proton conduction,[17] this barrier alone, does not seem sufficient to fully explain the low proton conductance rate.[33,34,55,59,60] Recently, Markiewicz et al.[26] provided experimental evidence indicating that the Trp41 tetrad is mostly dehydrated even under acidic conditions, which suggests the existence of a second barrier on the proton-conducting pathway, due to the discontinuity between water clusters B and C (Supporting Information, Figure S1). In other words, for a proton released from His37 to water cluster B an additional conformational change, besides that of His37, is required to pass the proton through the

Trp41 gate.[24] Therefore, we believe that the inter-helical motion captured by PET, the rate of which matches the upper limit of the observed proton conductance rate, not only necessitates proton conduction but also controls its flux. This picture is further supported by electrophysiological studies that show the conduction of the channel increases at low pH, even after correcting for the increase in the permeant ion concentration gradient.[56,61] In addition, our observation that τ_{PET} becomes smaller at acidic pH compared to that at basic pH is consistent with experimental[17,23,47,48] and simulation[36,59,62,63] studies showing that the M2 tetrameric assembly is more dynamic at low pH. For example, the study of Schnell and Chou[4] found that the dynamics of the Trp41 sidechain is significantly increased when the pH is decreased from 7.5 to 6.0 and that lowering the pH from 7.5 to 6.5 broadens most of the NMR resonances corresponding to the TM helix. The latter suggests pH-dependent inter-helical motion.

In summary, we have taken advantage of the fact that a Trp residue can quench the florescence of a nearby Atto 655 dye and employed this quencher-fluorophore pair to interrogate the inter-helical motion of the M2 proton channel through the Trp41 gate, using fluorescence correlation spectroscopy. Our results have revealed that the time constant of this motion is in the range of tens to hundreds of microseconds and exhibits a sigmoidal dependence on pH in the range of 5 – 8. For the full-length M2 proton channel, the corresponding pH titration curve is manifested by a transition midpoint of 6.1, a high-pH baseline amplitude of 185 μs and a low-pH baseline amplitude of 84 μs. Because the midpoint of this pH titration curve is similar to the electrophysiologically observed conducting pK_a of the His37 gate, we believe that the corresponding inter-helical motion is coupled to proton conduction. Finally, as the rate of this motion is significantly slower than the equilibration rate between viral exterior and the His37 tetrad, it likely acts as a dynamic gate to further assist protons released from His37 to pass the Trp41 region before entering the interior of the virus.

Supplementary Material

Refer to Web version on PubMed Central for supplementary material.

Acknowledgments

References

1. Pinto LH, Lamb RA. J. Biol. Chem. 2006; 281:8997–9000. [PubMed: 16407184]

2. Shimbo K, Brassard DL, Lamb RA, Pinto LH. Biophys. J. 1996; 70:1335–1346. [PubMed: 8785289]

3. Hay AJ, Wolstenholme AJ, Skehel JJ, Smith MH. EMBO J. 1985; 4:3021. [PubMed: 4065098]

4. Schnell JR, Chou JJ. Nature. 2008; 451:591–595. [PubMed: 18235503]

5. Pielak RM, Schnell JR, Chou JJ. Proc. Natl. Acad. Sci. U.S.A. 2009; 106:7379–7384. [PubMed: 19383794]

6. Cady SD, Schmidt-Rohr K, Wang J, Soto CS, DeGrado WF, Hong M. Nature. 2010; 463:689–692. [PubMed: 20130653]

7. Balannik V, Carnevale V, Fiorin G, Levine BG, Lamb RA, Klein ML, DeGrado WF, Pinto LH. Biochemistry. 2010; 49:696–708. [PubMed: 20028125]

8. Wu Y, Canturk B, Jo H, Ma C, Gianti E, Klein ML, Pinto LH, Lamb RA, Fiorin G, Wang J, DeGrado WF. J. Am. Chem. Soc. 2014; 136:17987–17995. [PubMed: 25470189]

9. Pielak RM, Chou JJ. BBA-Biomembranes. 2011; 1808:522–529. [PubMed: 20451491]

10. Sansom MSP, Kerr ID, Smith GR, Son HS. Virology. 1997; 233:163–173. [PubMed: 9201226]

11. Smondyrev AM, Voth GA. Biophys. J. 2002; 83:1987–1996. [PubMed: 12324417]

12. Kass I, Arkin IT. Structure. 2005; 13:1789–1798. [PubMed: 16338407]

13. Pinto LH, Dieckmann GR, Gandhi CS, Papworth CG, Braman J, Shaughnessy MA, Lear JD, Lamb RA, DeGrado WF. Proc. Natl. Acad. Sci. U.S.A. 1997; 94:11301–11306. [PubMed: 9326604]

14. Gandhi CS, Shuck K, Lear JD, Dieckmann GR, DeGrado WF, Lamb RA, Pinto LH. J. Biol. Chem. 1999; 274:5474–5482. [PubMed: 10026160]

15. Schweighofer KJ, Pohorille A. Biophys. J. 2000; 78:150–163. [PubMed: 10620282]

16. Fiorin G, Carnevale V, DeGrado WF. Science. 2010; 330:456–458. [PubMed: 20966238]

17. Hu F, Luo W, Hong M. Science. 2010; 330:505–508. [PubMed: 20966251]

18. Pielak RM, Chou JJ. J. Am. Chem. Soc. 2010; 132:17695–17697. [PubMed: 21090748]

19. Sharma M, Yi M, Dong H, Qin H, Peterson E, Busath DD, Zhou H-X, Cross TA. Science. 2010; 330:509–512. [PubMed: 20966252]

20. Hu F, Schmidt-Rohr K, Hong M. J. Am. Chem. Soc. 2012; 134:3703–3713. [PubMed: 21974716]

21. Pinto LH, Holsinger LJ, Lamb RA. Cell. 1992; 69:517–528. [PubMed: 1374685]

22. Chizhmakov IV, Geraghty FM, Ogden DC, Hayhurst A, Antoniou M, Hay AJ. J. Physiol. 1996; 494:329–336. [PubMed: 8841994]

23. Williams JK, Zhang Y, Schmidt-Rohr K, Hong M. Biophys. J. 2013; 104:1698–1708. [PubMed: 23601317]

24. DiFrancesco ML, Hansen U-P, Thiel G, Moroni A, Schroeder I. PLOS One. 2014; 9:e107406. [PubMed: 25211283]

25. Zhou H-X. Biophys. J. 2011; 100:912–921. [PubMed: 21320435]

26. Markiewicz BN, Lemmin T, Zhang W, Ahmed IA, Jo H, Fiorin G, Troxler T, DeGrado WF, Gai F. PCCP. 2016; 18:28939–28950. [PubMed: 27725984]

27. Doose S, Neuweiler H, Sauer M. Chem Phys Chem. 2005; 6:2277. [PubMed: 16224752]

28. Marmé N, Knemeyer JP, Sauer M, Wolfrum J. Bioconjugate Chem. 2003; 14:1133.

29. Doose S, Neuweiler H, Sauer M. Chem Phys Chem. 2009; 10:1389–1398. [PubMed: 19475638]

30. Ding B, Hilaire MR, Gai F. J. Phys. Chem. B. 2016; 120:5103–5113. [PubMed: 27183318]

31. Rogers JMG, Polishchuk AL, Guo L, Wang J, DeGrado WF, Gai F. Langmuir. 2011; 27:3815–3821. [PubMed: 21401044]

32. Ma C, Polishchuk AL, Ohigashi Y, Stouffer AL, Schön A, Magavern E, Jing X, Lear JD, Freire E, Lamb RA, DeGrado WF, Pinto LH. Proc. Natl. Acad. Sci. U.S.A. 2009; 106:12283–12288. [PubMed: 19590009]

33. Acharya R, Carnevale V, Fiorin G, Levine BG, Polishchuk AL, Balannik V, Samish I, Lamb RA, Pinto LH, DeGrado WF, Klein ML. Proc. Natl. Acad. Sci. U.S.A. 2010; 107:15075–15080. [PubMed: 20689043]

34. Stouffer AL, Acharya R, Salom D, Levine AS, Di Costanzo L, Soto CS, Tereshko V, Nanda V, Stayrook S, DeGrado WF. Nature. 2008; 451:596–599. [PubMed: 18235504]

35. Stouffer AL, Nanda V, Lear JD, DeGrado WF. J. Mol. Biol. 2005; 347:169–179. [PubMed: 15733926]

36. Yi M, Cross TA, Zhou H-X. Proc. Natl. Acad. Sci. U.S.A. 2009; 106:13311–13316. [PubMed: 19633188]

37. Hu J, Fu R, Nishimura K, Zhang L, Zhou H-X, Busath DD, Vijayvergiya V, Cross TA. Proc. Natl. Acad. Sci. U.S.A. 2006; 103:6865–6870. [PubMed: 16632600]

38. Buschmann V, Weston KD, Sauer M. Bioconjugate Chem. 2003; 14:195–204.

39. Tcherkasskaya O, Ptitsyn OB, Knutson JR. Biochemistry. 2000; 39:1879–1889. [PubMed: 10677239]

40. Clayton AHA, Sawyer WH. Biophys. J. 2000; 79:1066–1073. [PubMed: 10920036]

41. Henriksen J, Rowat AC, Brief E, Hsueh YW, Thewalt JL, Zuckermann MJ, Ipsen JH. Biophys. J. 2006; 90:1639–1649. [PubMed: 16326903]

42. Orädd G, Shahedi V, Lindblom G. BBA-Biomembranes. 2009; 1788:1762–1771. [PubMed: 19573518]

43. Cooper RA. J. Cell. Biochem. 1978; 8:413–430.

44. Gracia RS, Bezlyepkina N, Knorr RL, Lipowsky R, Dimova R. Soft Matter. 2010; 6:1472–1482.

45. Genova J, Bivas I, Marinov R. Colloids Surf. Physicochem. Eng. Aspects. 2014; 460:79–82.

46. Cristian L, Lear JD, DeGrado WF. Proc. Natl. Acad. Sci. U.S.A. 2003; 100:14772–14777. [PubMed: 14657351]

47. Miao Y, Fu R, Zhou H-X, Cross TA. Structure. 2015; 23:2300–2308. [PubMed: 26526851]

48. Li C, Qin H, Gao FP, Cross TA. BBA-Biomembranes. 2007; 1768:3162–3170. [PubMed: 17936720]

49. Okada A, Miura T, Takeuchi H. Biochemistry. 2001; 40:6053–6060. [PubMed: 11352741]

50. Colvin MT, Andreas LB, Chou JJ, Griffin RG. Biochemistry. 2014; 53:5987–5994. [PubMed: 25184631]

51. Liao SY, Yang Y, Tietze D, Hong M. J. Am. Chem. Soc. 2015; 137:6067–6077. [PubMed: 25892574]

52. Wang C, Lamb RA, Pinto LH. Biophys. J. 1995; 69:1363–1371. [PubMed: 8534806]

53. Hong M, DeGrado WF. Prot. Sci. 2012; 21:1620–1633.

54. Ma C, Fiorin G, Carnevale V, Wang J, Lamb RA, Klein ML, Wu Y, Pinto LH, DeGrado WF. Structure. 2013; 21:2033–2041. [PubMed: 24139991]

55. Mould JA, Li H-C, Dudlak CS, Lear JD, Pekosz A, Lamb RA, Pinto LH. J. Biol. Chem. 2000; 275:8592–8599. [PubMed: 10722698]

56. Lin T-I, Schroeder C. J. Virol. 2001; 75:3647–3656. [PubMed: 11264354]

57. Moffat JC, Vijayvergiya V, Gao PF, Cross TA, Woodbury DJ, Busath DD. Biophys. J. 2008; 94:434–445. [PubMed: 17827230]

58. Decoursey TE. Physiol. Rev. 2003; 83:475–579. [PubMed: 12663866]

59. Khurana E, Peraro MD, DeVane R, Vemparala S, DeGrado WF, Klein ML. Proc. Natl. Acad. Sci. U.S.A. 2009; 106:1069–1074. [PubMed: 19144924]

60. Yi M, Cross TA, Zhou H-X. J. Phys. Chem. B. 2008; 112:7977–7979. [PubMed: 18476738]

61. Chizhmakov IV, Ogden DC, Geraghty FM, Hayhurst A, Skinner A, Betakova T, Hay AJ. J. Physiol. 2003; 546:427–438. [PubMed: 12527729]

62. Liang R, Swanson JMJ, Madsen JJ, Hong M, DeGrado WF, Voth GA. Proc. Natl. Acad. Sci. U.S.A. 2016; 113:E6955–E6964.

63. Wei C, Pohorille A. Biophys. J. 2013; 105:2036–2045. [PubMed: 24209848]
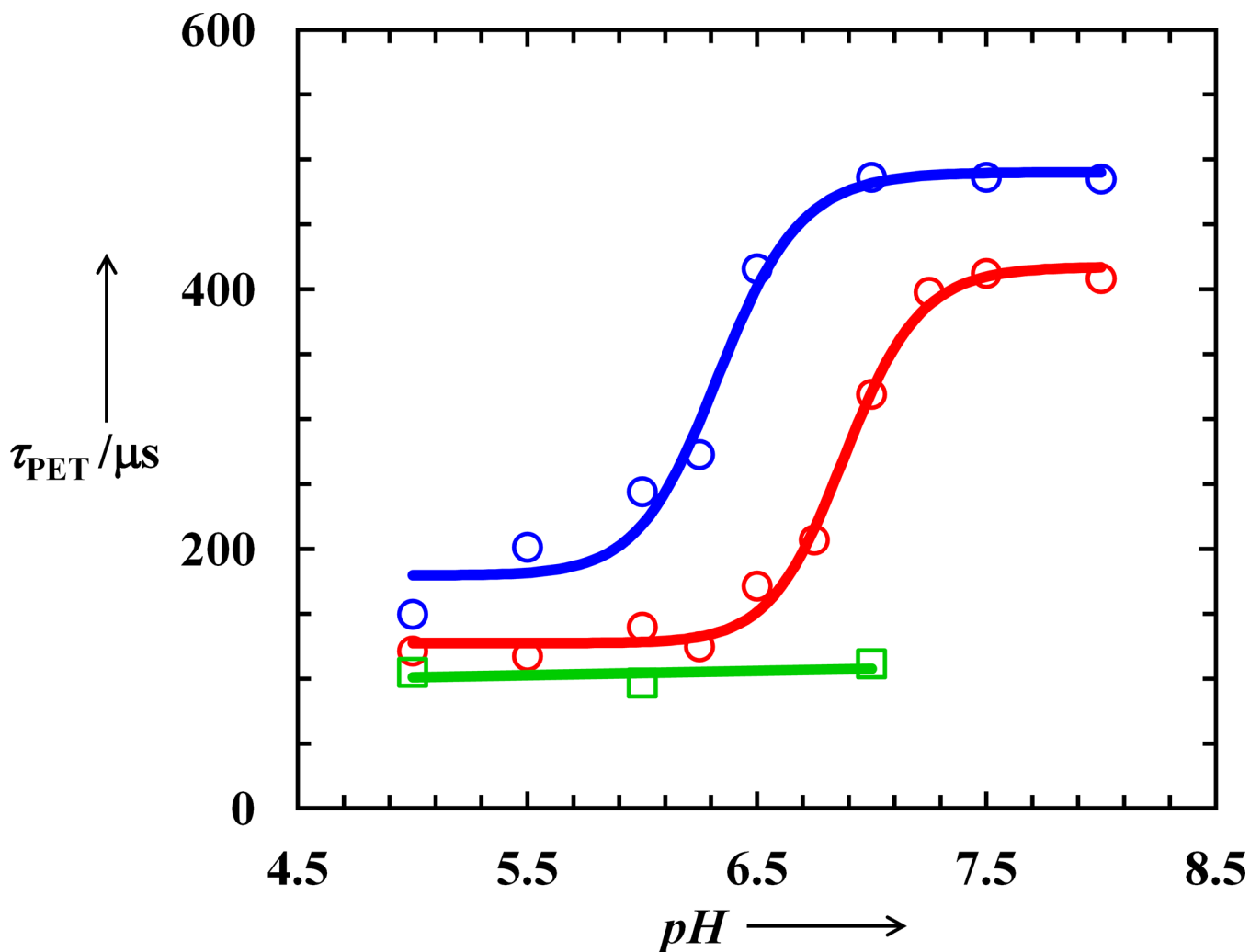
Figure 1.
Dependence of the PET time component (τ_{PET}) on pH for M2TM*-M2TM channels in LUVs consisting of POPC/POPG (4/1) (blue cycles) or POPC/POPG/Cholesterol (4/1/2) (red cycles). The solid line in each case corresponds to the best fit of the data to a Hill equation and the resultant midpoint pH value is 6.8 ± 0.1 for POPC/POPG LUV and 6.3 ± 0.2 for POPC/POPG/Cholesterol LUV respectively. Also shown is the pH dependence of τ_{PET} obtained for M2TM*-His37/Gly M2TM channels in LUV membranes consisting of POPC/POPG/Cholesterol (4/1/2) (green squares).
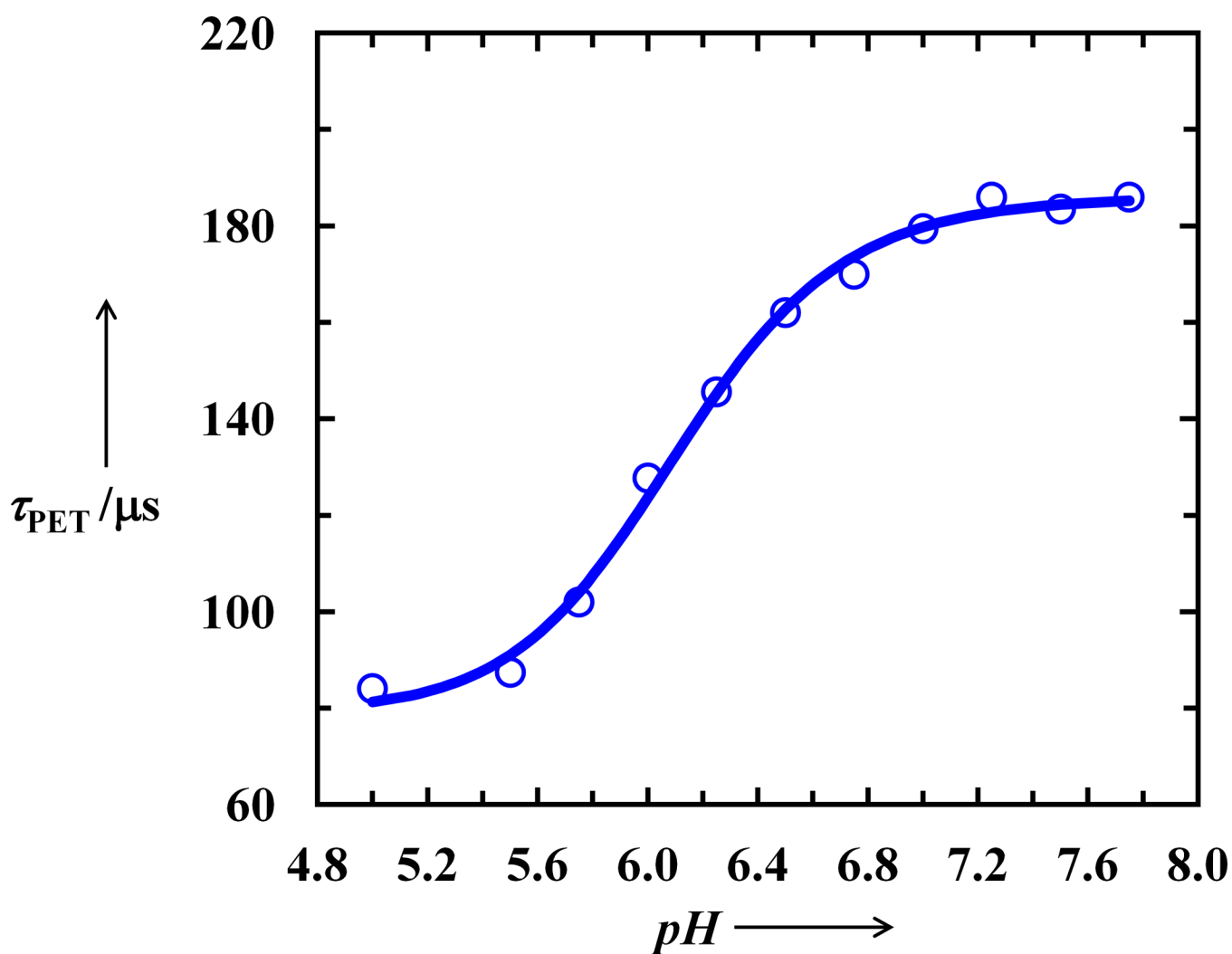
Figure 2.
Dependence of the PET time constant (τ_{PET}) on pH for M2*-M2 channels in LUVs
consisting of POPC/POPG/Cholesterol (4/1/2). The solid line corresponds to the best fit of
the data to a Hill equation and the resultant midpoint pH value is 6.1 ± 0.2.